

Origin of crystallization-induced refractive index changes in photo-thermo-refractive glass

Julien Lumeau^{a,*}, Larissa Glebova^a, Valerii Golubkov^b, Edgar D. Zanotto^c, Leonid B. Glebov^a

^a CREOL/University of Central Florida, 4000, Central Florida Blvd., Orlando, FL 32816-2700, USA

^b Institute of Silicate Chemistry, Russian Academy of Science, St. Petersburg 199155, Russia

^c Vitreous Materials Laboratory, LaMaV, Department of Materials Engineering, DEMa, Federal University of São Carlos, UFSCar, 13565-905 São Carlos, SP, Brazil

ARTICLE INFO

Article history:

Received 12 December 2008

Received in revised form 18 May 2009

Accepted 1 July 2009

Available online 8 August 2009

PACS:

13.42.70.Ce

14.42.40.Eq

15.61.46.Hk

78.20.Ci

81.40.Jj

Keywords:

Crystallization

Refractive index change

Photosensitivity

Optical glass

Stress

ABSTRACT

Photo-thermo-refractive (PTR) glass is a multi-component silicate that undergoes localized refractive index decrease after UV-exposure and thermal treatment for partial crystallization. Based on this refractive index change, high efficiency volume Bragg gratings have been developed in PTR glass and have been successfully used for laser beam control. However, despite the fact that this type of glass has been widely studied and used over the last 20 years, the *origin* of the refractive index change upon crystallization is poorly understood. In this paper, we introduce three possible mechanisms (the precipitation of nano-sized NaF crystals and the associated local chemical changes of the glass matrix, the volumetric changes due to relaxation, and the local residual stresses) for the refractive index decrement in PTR glass and estimate the partial refractive index change due to each mechanism. Refractive index measurements are compared with high temperature XRD experiments and a general approach for the simulation of the refractive index change in PTR glass is proposed. We show that among the studied variables the residual stresses surrounding the crystals are the main responsible for the local refractive index decrement in this glass.

© 2009 Elsevier B.V. All rights reserved.

1. Introduction

Photo-thermo-refractive (PTR) glass is a sodium–potassium–zinc–aluminum–fluorine–bromine silicate glass doped with antimony, tin, cerium, and silver. This class of glasses, which undergo photo-thermo-induced crystallization, was invented by Stookey [1] many years ago and has been studied as a candidate for hologram writing in the last 20 years [2–5]. PTR glass exhibits a localized refractive index change after UV-exposure and successive thermal treatment above the glass transition temperature, T_g , which results from the crystallization of about 0.1 wt% sodium fluoride nano-crystals [6]. The possibility of recording phase holograms in this glass has potential for many high-tech applications, such as optical filtering [7] and spectral beam combining of high power lasers [8].

A description of the complex photo-thermo-induced crystallization mechanisms in this type of glass is given in Ref. [9]. The evolution of the material's nanostructure and optical properties after

UV-exposure and thermal treatment are reported in several publications e.g. [6,10–14]. However, despite the advanced knowledge about PTR glass and its numerous commercial and potential applications, the *origin* of the (local) refractive index change after UV-exposure and thermal treatment is still unclear.

It was shown in Ref. [6] that the photosensitivity of PTR glass results from the precipitation of nano-sized sodium fluoride crystals within the glass matrix in the UV-exposed regions after heat treatment. However, it is not clear which particular structural transformations are responsible for the refractive index decrement in such complex multi-component glass. The understanding of the origin of this effect requires a step by step discussion of the mechanisms of photosensitivity in PTR glass. A *simplified* proposal for photo-thermal crystallization is the following: before any thermal development of the glass, sodium, fluorine and all other ions are uniformly dissolved in the matrix and the material is totally vitreous. When PTR glass is exposed to long wavelength UV radiation $\lambda > 250$ nm (e.g. He–Cd laser at 325 nm), Ce^{3+} releases an electron and converts to hole-type Ce^{4+} center. The released electron is then trapped by intrinsic defects of the glass matrix or dopants and impurities in the highest valence state, including silver ions

* Corresponding author. Tel.: +1 321 948 5115.

E-mail address: jlumeau@creol.ucf.edu (J. Lumeau).

dispersed in the glass matrix. Then silver ions convert to silver atoms. When a UV-exposed glass is nucleated at temperatures between 450 and 500 °C, silver atoms agglomerate and form colloidal silver. Another possibility is that silver bromide clusters form [15]. The second part of the crystallization process consists in the heterogeneous precipitation and growth of sodium fluoride crystals on top of the silver (or silver bromide) clusters. NaF growth is then controlled by diffusion of sodium and fluorine from the glass matrix to the crystals, which leave sodium and fluorine depleted regions surrounding each crystal [16]. Thus a simplified model for PTR glass after UV-exposure and heat-treatment supposes that three distinct areas appear (Fig. 1):

- The first area is a cubic sodium fluoride crystal (shown here as a sphere for simplicity of modeling). For typical conditions of UV-exposure and thermal development used for hologram recording, the average diameter of such crystals is about 20 nm [12] and their volume fraction is about 0.1% [6]. This means that the average distance between crystals is about 110 nm.
- As sodium and fluorine ions are consumed by the growing crystals, halos with diameter about three times larger than the crystal diameter have the same components as virgin PTR glass, but are depleted in sodium and almost exhausted in fluorine.
- The third area, far away from the crystals, is an unperturbed glass region having identical composition as virgin PTR glass.

The precipitation of sodium fluoride crystals correlates with the beginning of the refractive index decrease in the UV-exposed regions of the glass. It must be stressed that a (smaller) change of refractive index also occurs in the unexposed areas [17]. However, as the main application of PTR glass is for recording volume Bragg gratings, the important parameter is the refractive index difference between the UV-exposed area ($n^{\text{UV-exposed}}$) and the unexposed area ($n^{\text{unexposed}}$):

$$\Delta n = n^{\text{UV-exposed}} - n^{\text{unexposed}} \quad (1)$$

It has been found [2,10] that the overall refractive index change is negative ($\Delta n < 0$), therefore, PTR glass is a negative photosensitive medium.

Based on the above description, it is possible to write a phenomenological equation describing possible contributions to the refractive index decrement in both UV-exposed and unexposed areas. For simplification, we supposed that all contributions are additive and we dropped integrals that would take into account an inhomogeneous distribution of each contribution:

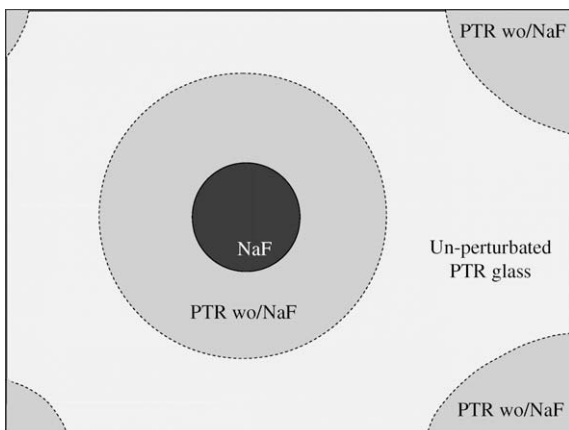


Fig. 1. Three-phase structure of PTR glass after successive UV-exposure and thermal treatment.

$$\begin{aligned} \Delta n^{\text{exp}} = & \left[\Delta n^{\text{crystalline}} V^{\text{NaF}} + \Delta n^{\text{vitreous}} V^{\text{PTR wo NaF}} \right] \\ & + \left[\Delta n^{\text{V}} V^{\text{PTR wo NaF}} + \Delta n^{\text{V}'} V^{\text{PTR w NaF}} \right] \\ & + \left[\Delta n^{\text{stress1}} V^{\text{NaF}} + \Delta n^{\text{stress2}} V^{\text{PTR wo NaF}} + \Delta n^{\text{stress3}} V^{\text{PTR w NaF}} \right] \end{aligned} \quad (2)$$

By supposing that there is no significant crystallization in the unexposed areas, the refractive index in those areas would change only due to variations of cooling regimes (which is different from the one used for fine annealing of the glass and results in volumetric changes associated with glass relaxation):

$$\Delta n^{\text{unexp}} = \Delta n^{\text{V}'} \times V^{\text{PTR w NaF}} \quad (3)$$

Each contribution in Eqs. (2) and (3) is a product (or integration) between the refractive index change (Δn^i) due to each effect and the volume fraction (V^i) of the region contributing to that particular effect. V^{NaF} is the volume fraction of crystals – which is typically between 0.01% and 0.1% – $V^{\text{PTR wo NaF}}$ is the volume fraction of glass that has been depleted in sodium and fluorine, and $V^{\text{PTR w NaF}}$ is the volume fraction of glass that has not been perturbed and, therefore, has the same composition as regular PTR glass.

Let us now describe each one of these contributions. Regarding the refractive index change appearing after thermal treatment in UV-exposed areas, the first term within brackets represents the direct contribution of crystallization to the refractive index change. The appearance of sodium fluoride crystals induces a refractive index change ($\Delta n^{\text{crystalline}}$) due to their lower refractive index ($n = 1.32$) compared to the refractive index of the original glass matrix ($n \sim 1.5$). Moreover, one could expect that the atomic refractions of sodium and fluorine are different in the crystalline and vitreous phases. And this effect is accompanied by NaF depletion of the surrounding glass which, in turn, changes the refractive index of the glass matrix ($\Delta n^{\text{vitreous}}$).

The terms within the second bracket, Δn^{V} and $\Delta n^{\text{V}'}$, refer to changes of refractive index in the NaF depleted and unperturbed PTR glass, respectively, due to the change of specific volume that occurs during cooling of PTR glass (after crystallization treatment) in comparison with the specific volume of the virgin glass, which underwent fine annealing.

The third term represents the stresses that appear in the NaF crystals, surrounding glass and unperturbed glass. Crystallization is typically performed at ~ 515 °C. PTR “glass” is a viscous liquid at this temperature because $T_g \sim 460$ °C and, therefore, stresses caused by structural transformations quickly relax. But when the material is cooled down from T_g to ~ 25 °C, stresses appear in the elastic medium (glass).

It is known that the coefficient of thermal expansion (CTE, α) of silicate glasses increases with an increase of the fluorine content [18]. Hence we have:

$$\alpha_{\text{PTR wo NaF}} < \alpha_{\text{PTR w NaF}} < \alpha_{\text{NaF}} \quad (4)$$

The coefficient of thermal expansion (CTE) of regular PTR glass is $\sim 10 \times 10^{-6} \text{ K}^{-1}$, while that of the cubic NaF crystals is $\sim 36 \times 10^{-6} \text{ K}^{-1}$, i.e. almost four times higher than the glass CTE. Hence, after crystallization and cooling down to room temperature, “hydrostatic” radial and tangential stresses appear within the NaF crystals and induce a refractive index change on them ($\Delta n^{\text{stress1}}$) [19], radial and tangential stresses change the refractive index of the surrounding glass ($\Delta n^{\text{stress2}}$) [19], and finally there will be some stresses between the depleted and unperturbed glass ($\Delta n^{\text{stress3}}$). The spatial distribution of these stresses is not uniform. The stresses inside the NaF crystals are constant, while the stresses in the depleted and non-depleted Na and F regions decay with the distance, r^{-3} . Moreover, due to the much larger difference in thermal expansion coefficients, the main contribution is expected to be the

stresses at the interface between NaF crystals and surrounding (fluorine and sodium depleted) glass. The total contribution of each type of stresses to the refractive index change is a volume integral across the areas occupied by these stresses.

Regarding the unexposed (supposedly non-crystallized) parts of the glass, only the change of specific volume during cooling from the crystallization temperature to room temperature could contribute to the refractive index change. However, unpublished results confirm that in addition to copious nucleation in the UV-exposed regions, there is also some (less intense) crystallization in unexposed parts of PTR glass. But in this study we reasonably assume that such crystallization in unexposed regions at the standard regime of thermal development is negligible.

The above described (simplified) structural changes in PTR glass with UV-exposure and thermal treatment are rather complex, but should be understood for further development and improvement of efficient optical elements based on PTR glass. Hence, this paper aims to quantify some possible contributions to the local refractive index change upon UV-exposure and thermal treatment.

For that purpose we measured and extracted the effect of precipitation of nano-sized NaF crystals and the associated local chemical changes of the glass matrix, the effect of glass relaxation and finally the effect of the local residual stresses around the crystals by measuring the change of PTR glass properties “in situ” at high temperatures. Then, we propose a model for the refractive index decrement in this glass and show the dominant role of *residual stresses*.

2. Experimental – materials and methods

2.1. Glass sample preparation

Samples of a photosensitive PTR glass containing $15\text{Na}_2\text{O}-5\text{ZnO}-4\text{Al}_2\text{O}_3-70\text{SiO}_2-5\text{NaF}-1\text{KBr}-0.01\text{Ag}_2\text{O}-0.01\text{CeO}_2$ (mol%) and similar minor amounts of Sn and Sb were used in this work, as in previous studies [3–6]. The glass was melted in an electric furnace in a 0.5 liter platinum crucible at 1460°C for 5 h in air. Stirring with a Pt blade was used to homogenize the liquid. After melting, homogenizing and fining, the glass was cooled to the glass transition temperature ($T_g \sim 460^\circ\text{C}$), then annealed at T_g for 2 h, and cooled to room temperature at a rate of 0.1 K/min.

To study the effect of the local chemical changes on refractive index decrease in PTR glass a common soda-lime-silica glass with the following composition: $3\text{CaO}-22\text{Na}_2\text{O}-75\text{SiO}_2$ was melted. The glass preparation procedure was identical to the one used for PTR glass except the annealing temperature that was increased to 560°C . In order to study the effect of fluorine on the absolute refractive index of PTR glass, new soda-lime-silica glasses were melted with different amounts of fluorine and using the same procedure than for the regular soda-lime-silica glass. These glasses were formulated with constant atomic concentration of cations (Na, Ca and Si), while O was substituted with F by equimolar substitution of Na_2O with $(\text{NaF})_2$.

Polished $25 \times 25 \times 2 \text{ mm}^3$ samples were prepared from each batch. The chemical homogeneity of the samples is a critical parameter affecting both optical and crystallization properties [20], thus homogeneity was quantified by measurements using an interferometer (GPI Zygo). The samples selected for this study had refractive index fluctuations of less than 40 ppm (peak-to-valley) across the aperture, i.e. these samples are considered of excellent optical quality.

2.2. Refractive index measurements

Two different quantities were measured. The first one is the absolute refractive index of the soda-lime-silica samples. A con-

ventional Abbe refractometer was used to carry out this measurement. The estimated precision of each measurement was in the ± 200 ppm range.

The second quantity is the refractive index change (photosensitivity) in PTR glass that resulted from UV-exposure and thermal treatment. The method used was the same as in Ref. [10]. Glass samples for refractive index measurements were fixed onto a computer-controlled translation stage and moved across a laser beam (He-Cd laser, 4 mW, 325 nm) at constant velocity in order to record a stripe with controlled distribution of dosages (Gaussian distribution with maximum of 0.9 J/cm^2). After exposure, the samples were thermally developed for 30 min at 520°C . Refractive index changes were measured in each sample using a shearing interferometer setup [10]. Its basic principle is to create an interferogram that converts the phase change at propagation through the glass to a fringe shift. A liquid cell with an index matching fluid was used to prevent thickness variations of the sample which would contribute to fringe shift. Therefore the interferometer fringe distortions resulted only from refractive index variations.

2.3. X-ray diffraction measurements

X ray diffraction (XRD) was studied with the use of a Cu $K\alpha$ radiation [12]. The sample was fixed on a double-sided adhesive tape and placed on the sample holder. The whole assembly was finally inserted into the chamber for the angular distribution of XRD measurement and crystalline phase determination. Measurements could not be performed over a wide angular range. As a matter of fact, while three distinct peaks assigned to NaF crystals can be measured in PTR glass when all NaF is crystallized in the glass, only the peak between 38° and 39° can be detected in glasses that were developed for short duration at $\sim 520^\circ\text{C}$, as only ~ 0.01 – 0.1 vol% of NaF crystals are then present in the glass [6]. Therefore, to increase the integration time for each angle, we limited our measurements between 37.5° and 39.5° .

2.4. High temperature interferometry measurements

In order to study in situ the evolution of the refractive index while heating up the glass to up 550°C , a specific Michelson interferometer was constructed (Fig. 2). A 1-mm-beam of a He-Ne laser was expanded with a telescope to produce a large beam (about 20 mm) with a uniform intensity profile in its center. Then this large beam was split into two smaller beams using a pellicle beamsplitter. Each beam was reflected using two metallic mirrors, and the beams were then recombined by the beamsplitter. Interferences between these two beams were projected on a CCD camera and recorded with a video acquisition card. The two arms were

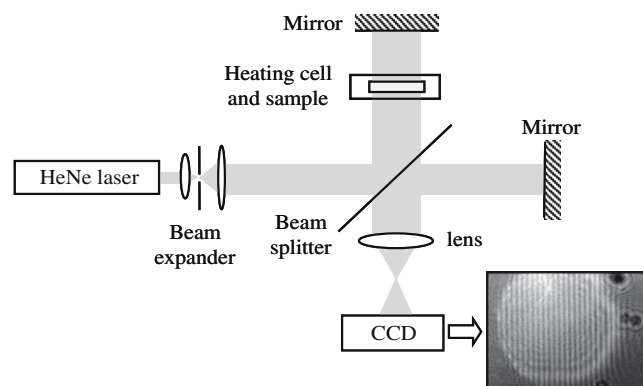


Fig. 2. A Michelson interferometer for the measurement of the refractive index change in UV exposed and developed PTR glass at different temperatures.

aligned to produce vertical plane parallel fringes on the CCD camera. A heating cell was finally inserted in one of the arms of the interferometer. The evolution of the refractive index change was studied by monitoring the evolution of the fringe shift where the sample was UV-exposed, the fringe shift being linearly linked to the change of the optical thickness of the studied sample.

3. Results

3.1. Estimation of the effect of chemical changes on the refractive index change

The local *chemical changes* that occur in PTR glass due to crystallization of NaF are the most straightforward, however, two effects occur concurrently: the first is the refractive index change due to the appearance of NaF crystals, which leads to a local decrease of the refractive index due to their lower refractive index (1.326) than the refractive index of the original glass matrix (1.50). But a concurrent effect also occurs, i.e. a change of the composition of the glass region surrounding each crystal, which increases the local refractive index. In order to estimate this contribution, we determined the atomic refraction of “amorphous NaF” when dispersed in a glass matrix. This analysis was performed with soda-lime-silica glasses (3CaO 22Na₂O 75SiO₂) having different fluorine concentrations. The refractive index was measured in each of these glasses using an Abbe refractometer. The method of Demkina [21] was used to model the refractive index of each of these glasses. For each glass the refractive index n can be written as follows:

$$n = \frac{\frac{a_{\text{CaO}}}{s_{\text{CaO}}} n_{\text{CaO}} + \frac{a_{\text{SiO}_2}}{s_{\text{SiO}_2}} n_{\text{SiO}_2} + \frac{a_{\text{Na}_2\text{O}}}{s_{\text{Na}_2\text{O}}} n_{\text{Na}_2\text{O}} + \frac{a_{\text{NaF}}}{s_{\text{NaF}}} n_{\text{NaF}}}{\frac{a_{\text{CaO}}}{s_{\text{CaO}}} + \frac{a_{\text{SiO}_2}}{s_{\text{SiO}_2}} + \frac{a_{\text{Na}_2\text{O}}}{s_{\text{Na}_2\text{O}}} + \frac{a_{\text{NaF}}}{s_{\text{NaF}}}} \quad (5)$$

where a_i are the weight percentage of each oxide and fluoride compounds, s_i , their molar mass and n_i their atomic refraction. All these parameters are tabulated and can be found in Ref. [21], except for the atomic refraction of NaF, which is the parameter of interest. We thus fitted the experimental data (refractive index versus NaF concentration) by optimizing the atomic refraction of NaF (Fig. 3) and found that for “amorphous NaF”, $n_{\text{NaF}} \sim 1.34 \pm 0.03$. This is thus about the same as the refractive index of crystalline NaF.

3.2. Estimation of the effect of specific volume change on the refractive index change

The second possible source of refractive index change after thermal treatment is the change of the specific volume of the glass

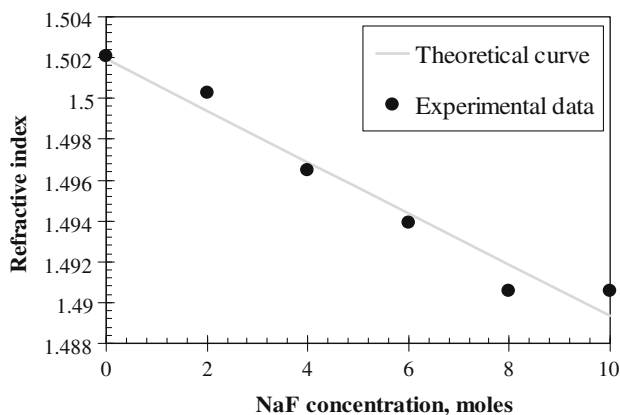


Fig. 3. Dependence of refractive index of fluorine doped soda-lime-silica glass on fluorine concentration.

caused by the cooling from the crystallization temperature of 520 °C. To illustrate this effect, we revisited some of the results presented in Ref. [17]. The evolution of refractive index was measured in two different PTR glasses, in both unexposed and UV-exposed areas; before and after thermal treatment (Table 1). These two PTR glasses were the following. The first one was a glass without bromine, and the second a regular PTR glass. The advantage of using bromine-free PTR glass is that it has the same photo-chemistry as regular PTR glass, but no crystallization can be detected after a regular heat-treatment. Table 1 shows that the refractive index decreases by several hundreds of ppm in both UV-exposed and unexposed areas of bromine-free PTR glass. This result illustrates the effect of volume change on the refractive index in PTR glass. Also, within the error limits (± 200 ppm), the change is the same in both unexposed and UV-exposed area if no crystallization occurs. More precise measurements using an interferometric setup [10] confirmed that refractive indices in unexposed and UV-exposed area are equal within the measurement error (± 10 ppm). Measurements in regular PTR glass show that this change of refractive index due to volume change also appears when crystallization is present, and that an additional effect due to residual stresses induces a larger refractive index change in the UV-exposed area.

3.3. Effect of temperature (residual stresses) on X-ray diffraction spectra of partially crystallized PTR glass

The effect of an increase of temperature (and residual stresses) on the X-ray diffraction spectra of PTR glass was studied (as shown in Ref. [6], at room temperature the XRD peak of these crystals is shifted to smaller angles). A regular PTR glass was UV-exposed and then thermally developed for about 1 h at 515 °C to precipitate NaF nano-crystals. Then this sample was coated with a thin layer of NaF crystal powder. It was found that this sample demonstrates two separated peaks (20 °C curve in Fig. 4) which could be assigned to NaF crystals in equilibrium (powder) and stretched NaF crystals in glass volume. Then X-ray diffraction spectra were obtained for different temperatures: 200, 350 and 500 °C. As can be seen, the two peaks shift to lower angle and tend to become a single one when the temperature reaches 500 °C. At this temperature, NaF crystals in bulk and on surface of the glass have identical properties, showing the residual stresses are relieved while heating the glass to temperature above T_g .

3.4. Effect of temperature (residual stresses) on the refractive index change

The effect of an increase of temperature on the photo-thermo-refractive index change was studied using a custom Michelson interferometer. A PTR glass sample that was previously UV-exposed with a Gaussian stripe and thermally developed for 1 h at 515 °C to induce refractive index change was inserted in the heating cell that was then inserted in one arm of the interferometer. The original refractive index change between exposed and unexposed areas at room temperature was ~ 450 ppm. Then the cell was heated up to 540 °C and the evolution of the interferogram

Table 1

Absolute refractive index in regular and bromine-free PTR glass before and after thermal development; for UV-exposed and unexposed samples.

Br Concentration, mol%	0	1
Refractive index		
Virgin, n_0	1.4967	1.4982
Developed unexposed, n_d	1.4964	1.4979
Developed UV-exposed, n_{dUV}	1.4962	1.4970
$n_d - n_0$, ppm	-300	-300
$n_{dUV} - n_0$, ppm	-500	-1200

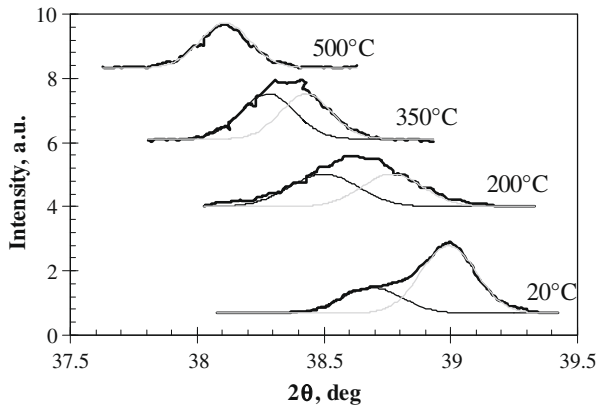


Fig. 4. XRD spectra measured on UV-exposed and developed PTR glass sample coated with NaF powder at different temperatures. The grey curves represent the decomposition of these spectra with two Gaussian functions that can be ascribed to diffraction peaks of NaF powder and NaF crystals precipitated in the volume of PTR glass.

with temperature is shown in Fig. 5. The fringe shift evolved and cancelled at some specific temperature. However, with such an interferometer, only the change of optical thickness is measured and it is not possible to easily decorelate the refractive index change to the modified physical thickness of the sample [11]. In order to figure out the contribution of glass swelling to the change of optical thickness when a sample is heated, we slightly modified the configuration of the setup shown in Fig. 2. The mirror behind the sample was removed and the back surface of the sample was ground to allow a single reflection from its front face. Then the PTR glass window was aligned such as this front face reflection interfered on the CCD camera with the reference beam. In that way we measured the distortion of the PTR glass surface at high temperature. Fig. 6 shows the interferograms measured at 450 °C and 550 °C. One can see that the direction of fringe distortions is different depending on the temperature of measurement demonstrating a change of sign of the glass swelling.

4. Discussion

Several different potential contributions to photo-thermo-refractive index change in PTR glass were investigated. Based on Eqs. (1) and (2), we supposed that three main effects can be considered. Other effects can originate a refractive index change in PTR

glass, such as the presence of liquid phase separation [16]. However, the discovery of these effects in PTR glass has only been reported recently and their role in the PTR glass photosensitivity is yet completely unknown. Therefore we limited our study to effects related to crystallization of NaF.

The first considered contribution is due to *compositional changes* of the glass matrix and the change of the material's structure from a vitreous state to a partially crystallized glass. To understand how the appearance of NaF crystals influences the refractive index of PTR glass, we calculated the molar refraction of “amorphous” NaF in glass (Fig. 3) and found that it is equal to $n_{\text{NaF}} \sim 1.34 \pm 0.03$. However, the refractive index of crystalline NaF is $n_{\text{NaF crystals}} \sim 1.326$, which is close to the atomic refraction of NaF in this oxide glass. This result indicates that when Na and F are converted into NaF crystals, the local decrease of the refractive index due to the crystals appearance is compensated by a similar increase of the refractive index of the NaF depleted regions in PTR glass and, therefore, the resulting (local) refractive index change due to the precipitation of NaF microcrystals is negligible. Thus NaF crystallization and the resulting change of chemistry of the glass is not the main effect leading to refractive index change in PTR glass.

The second possible source of photo-thermo-refractive index change in PTR glass is linked to *glass relaxation*. It is well-known that when a glass is heated at a temperature close to T_g it rapidly relaxes. The first time PTR glass enters this state is on cooling the liquid from the melting temperature down to T_g . PTR glass is typically annealed at $T_g \sim 460$ °C and then slowly cooled down to room temperature at 0.1 °C/min. This treatment results in a certain fictive temperature and specific volume of the glass. When PTR glass is heated up again above T_g to induce crystallization (at 520 °C) and the wanted refractive index change, the glass relax to its metastable equilibrium state for the second time. But after this second heat treatment, the glass is cooled down to room temperature using a different cooling rate, which is usually more than one order of magnitude faster than that used after the original PTR glass annealing. This change of cooling rate increases the specific volume of the PTR glass that results in a decrease of its overall refractive index. This effect was illustrated with the values of Table 1. It can be seen that the refractive index is the same in both unexposed and UV-exposed area if glass does not crystallize. Hence, the change of specific volume of the glass has only a limited effect on the photosensitive properties of PTR glass.

The third effect that appeared in Eq. (2) is associated with the *residual stresses*. As we have schematically shown in Fig. 1, when crystallization occurs, regions having different coefficients of ther-

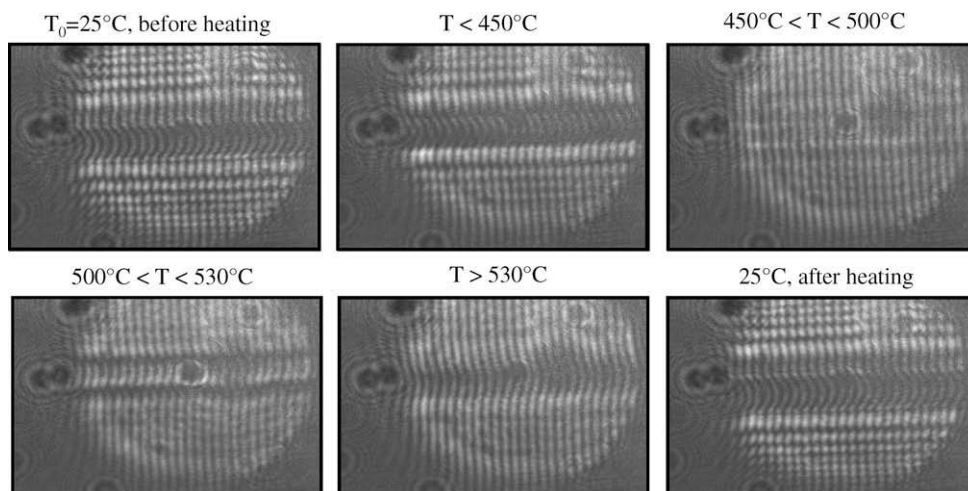


Fig. 5. Interferograms of a PTR glass sample exposed to a 1 mm Gaussian stripe of radiation at 325 nm and developed for 1 h at 515 °C.

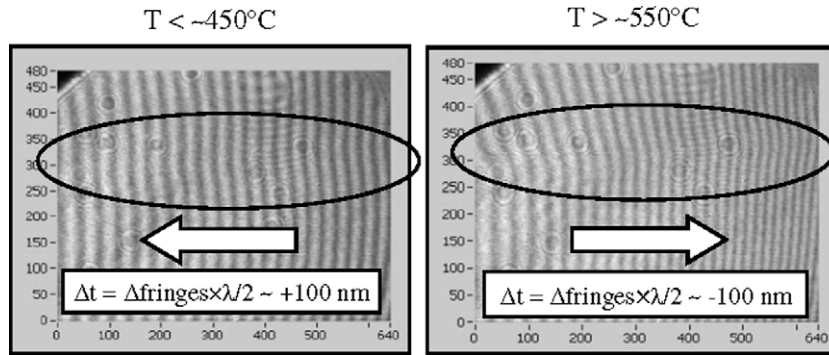


Fig. 6. Interferograms produced by a reflection from the front surface of PTR glass sample in a setup shown in Fig. 7.

mal expansion appear. Therefore, when the glass is cooled from its thermal treatment temperature (above T_g) to room temperature, stresses appear within the crystals and at the interfaces of the different regions. The residual stress within the NaF crystals was measured using NMR [22] and XRD [23] and was also estimated using the Selsing model [22,23]. Table 2 summarizes the values obtained by these different techniques. The notable fact is that the level of stress within each crystal is quite high (around 1 GPa!) and this is most likely the origin of the local variations of refractive index in PTR glass. When stress is applied to a glass it leads to elastic strain. This strain can be easily related to the refractive index change along all directions using the elasto-optic tensor of the overall glass. A refractive index change is, therefore, induced by stress through glass photoelasticity. But, as it will be discussed later, the real material is far more complex than the simple picture shown above and precise calculations of photoelastic refractive index increments would be a goal for future research.

After investigating the possible origins of the refractive index decrement in PTR glass and showing that residual stresses play a key role, we designed a set of experiments that permitted us to directly illustrate this dependence of refractive index change on stress. The first one consisted in measuring the evolution of the NaF diffraction peak of NaF crystals embedded in glass and comparing it to that of free NaF deposited on the sample's surface. As it was already mentioned, only very limited angular range were scanned because only one diffraction peak could be measured due to very low volume fraction of crystals embedded in the glass. Moreover, limiting the range of scanned angle allowed us to increase the integration time for each angle and, therefore, to significantly improve the signal to noise ratio. In order to analyze the evolution of the diffractograms, the diffraction peaks of the Fig. 4 were decomposed with two Gaussian functions with width corresponding to that in original diffraction pattern at room temperature. It is possible to assign the Gaussian function centered at lower angle to the NaF crystals present inside the PTR glass sample and the Gaussian function centered at the larger angle to the free NaF crystals deposited on the sample surface. On the diffractogram measured at room temperature the two peaks are separated. Then, when the temperature is increased, both peaks shift to lower an-

gles. Regarding the peak of the NaF crystals deposited on the surface, the shift can be explained by their thermal expansion coefficient; the increase of atomic spacing (d) when the temperature is increased results in a decrease of the diffraction angle based on Bragg's law:

$$n\lambda = 2d \sin(\theta) \Rightarrow \frac{\Delta d}{d} = \Delta\theta \cotan(\theta) = \alpha\Delta T \quad (6)$$

where n is an integer and λ the wavelength of the X-rays. A calculation based on the thermal expansion coefficient of NaF crystals gives a shift of the diffraction peak of $\sim 0.8^\circ$ for 480°C , which agrees with the measured value. Regarding the diffraction peak of bulk NaF crystals, at room temperature, the two peaks (shown with the Gaussian functions) are clearly distinct. This difference in position can be explained by the fact that when a crystal is stressed its Bragg angle shifts to lower angles [23]. Then, at 200°C the two peaks tend to get closer and to form only a broad diffraction peak. It means that the lattice parameters of the embedded and surface NaF crystals are closer. At higher temperatures the width of the overall diffraction peak decreases due to a decrease of the distance of the two fundamental peaks. At 500°C the width of the overall diffraction peak is minimal and coincides with the width of diffraction peak of the NaF powder deposited on the sample surface. This result means that the crystallographic properties of the bulk and surface NaF crystals are the same. This experiment gives a direct proof that there are no stresses surrounding the NaF crystals at high temperature and that these stresses are developed when the temperature is decreased down to room temperature.

The previous experiments demonstrated that the deviation of the lattice parameter of NaF precipitated in PTR glass from that of the free crystals increased as the temperature decreased. This phenomenon characterizes stresses in embedded NaF crystals. All these results mean that if stresses have a direct impact on the refractive index change and can be eliminated at high temperature ($>T_g$), the refractive index change could also be eliminated by heating up a PTR glass above T_g . We therefore measured the evolution of the optical thickness for different temperatures for a PTR glass which already exhibited a refractive index change (Fig. 5). But before performing any analysis of the evolution of the interferograms, it must be mentioned that before any heating, the lateral profile of the fringes almost follows the lateral profile of the exciting radiation. It is possible to show that the fringe shift is directly proportional to the change of optical thickness of the PTR glass window. Additionally to an interference pattern, there are horizontal bright lines of diffraction due to the contrast of refractive index between the UV-exposed stripes and the unexposed parts of the glass. When the temperature was increased up to 450°C , no significant change of the interferogram appeared. Then, when the temperature reached about 500°C , the interferogram changed significantly.

Table 2

Stresses at the interface between NaF crystals and surrounding glass in UV-exposed and thermally developed PTR glasses using different measurement techniques (NMR, XRD) and modeling).

Method	Stress	Tensile/compressive
Selsing model [19]	700 MPa	Tensile
XRD [20]	750–950 MPa	Tensile
NMR [19]	870 MPa	Tensile from F spectrum
	710 MPa	Tensile from Na spectrum

First, the magnitude of the fringe shift decreased, but the main effect was the disappearance of the diffraction lines. This effect means that even if there are still distortions of the fringes, these distortions are actually no longer due to the refractive index change, but due to a change of physical thickness. Actually, it was shown in Ref. [11] that the refractive index decrease in PTR glass is accompanied by an increase of the glass volume. It was also shown that this increase of volume appears in a broader area than the refractive index change. We therefore measured the change of the physical thickness of PTR glass at different temperatures (Fig. 6). At these temperatures the fringes are bended in opposite directions. This means that compared to the unexposed area of the glass, the surface of the exposed stripe is elevated at low temperatures, while it is lowered at higher temperatures. More precisely, a continuous monitoring of the interferogram revealed that below 450 °C there is no significant change. Between 450 °C and 520 °C, the fringe bending decreases, then disappears and finally changes direction. These data are quite relevant for the understanding the evolution of the refractive index change. Below 450 °C, there is almost no change in difference between exposed and unexposed areas for both the physical thickness and the refractive index. Then, when the glass is heated to the temperature normally used in the thermal development process, an elimination of the refractive index change occurs simultaneously with a decrease of the difference in the physical thickness between exposed and unexposed areas of the glass sample resulting in a similar shift of the fringes. But since a significant refractive index change no longer exists, diffraction of the probe beam disappears.

We have shown through PTR glass photo-elastic properties that residual stresses account for most of the refractive index change. Indeed, Eq. (4) shows that each of the different areas of the glass have different coefficients of thermal expansion, which result in the appearance of radial and tangential stresses in these areas after cooling the glass from the thermal development temperature to room temperature. Based on the difference of coefficients of thermal expansion and the scheme shown in Fig. 1, we represented in Fig. 7 the stress distribution in PTR glass. There is a very complex game of compressive and tensile radial and tangential stresses between different zones that result in an overall refractive index change [24]. More precisely, it can be shown that radial and tangential stresses exist inside the crystals (if they are considered as isotropic spherical particles) and are of equal magnitude. Moreover, this stresses state is “hydrostatic”. On the other hand, in the matrix (considered as an infinite isotropic medium), the tangential and radial stresses are different. The radial stresses are two times higher than the tangential stresses and have opposite sign from those inside the particle. Moreover both decrease with the cubic root of the distance from the particle [25].

Finally, as it was already mentioned, other possible effects, such as liquid–liquid phase separation, could contribute to the refractive index changes observed in PTR glass. This possibility and precise modeling of such structures is beyond the scope of this paper and should be further explored.

5. Conclusions

Main mechanisms of refractive index change in UV-exposed and thermally treated PTR glass were theoretically and experimentally investigated in this paper. Transformation of Na and F distributed in PTR glass matrix to crystalline NaF (chemical changes) and structural relaxation process are not the main causes of photo-thermo-induced refractive index changes. Such changes can be minimized or even eliminated by heating up the sample to a tem-

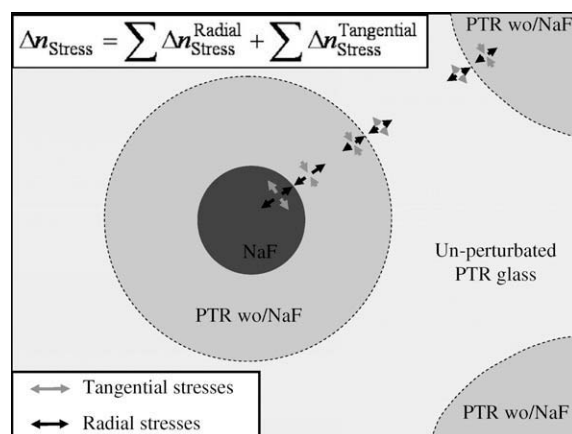


Fig. 7. Schematics of the distribution of stresses surrounding NaF crystals, Na and F depleted area of glass, and unperturbed glass.

perature exceeding T_g , as those normally used for thermal development of optical holographic elements. Among the variables here considered, the high residual stresses that surround the NaF crystals are the most important cause for photo-thermo-induced refractive index change in PTR glass.

Acknowledgements

This work was partially supported by DARPA contracts HR-01-1041-0004 and HR-0011-06-1-0010, and Brazilian funding agencies CNPq and Fapesp contract 2007/08179-9. The authors thank Prof. Francisco Serbena of UEPG, PR, Brazil, for his critical comments on stress distribution, Prof. W. Libardi of UFSCar, SP, Brazil for his help in understanding elasticity theory, and Dr Guilherme Souza and Dr. Vladimir Fokin of UFSCar, SP, Brazil for useful discussions.

References

- [1] S.D. Stookey, *Indust. Eng. Chem.* 41 (1949) 856.
- [2] V.A. Borgman, L.B. Glebov, N.V. Nikonorov, G.T. Petrovskii, V.V. Savvin, A.D. Tsvetkov, *Sov. Phys. Dokl.* 34 (1989) 1011–1013.
- [3] O.M. Efimov, L.B. Glebov, L.N. Glebova, K.C. Richardson, V.I. Smirnov, *Appl. Opt.* 38 (1999) 619.
- [4] O.M. Efimov, L.B. Glebov, S. Papernov, A.W. Schmid, in: *Laser-Induced Damage in Optical Materials*, Proc. SPIE, vol. 3578, 1999, p. 554.
- [5] O.M. Efimov, L.B. Glebov, V.I. Smirnov, *Opt. Lett.* 23 (2000) 1693.
- [6] T. Cardinal, O.M. Efimov, H.G. Francois-Saint-Cyr, L.B. Glebov, L.N. Glebova, V.I. Smirnov, *J. Non-Cryst. Solids* 325 (2003) 275–281.
- [7] L.B. Glebov, V.I. Smirnov, C.M. Stickley, I.V. Ciapurin, in: W.E. Tompson, P.H. Merritt (Eds.), *Laser Weapons Technology III*, Proceedings of SPIE, vol. 4724, 2002, pp. 101–109.
- [8] L.B. Glebov, *Phys. Chem. Glasses: Eur. J. Glass Sci. Technol. B* 48 (2007) 123–128.
- [9] D. Stookey, G.H. Beall, J.E. Pierson, *J. Appl. Phys.* 49 (1978) 5114.
- [10] O.M. Efimov, L.B. Glebov, H.P. Andre, *Appl. Optics* 41 (2002) 1864–1871.
- [11] L.B. Glebov, L. Glebova, *Glass Sci. Technol.* 75 (C2) (2002) 294–297.
- [12] L. Glebova, L. Glebova, V. Tsechomskii, V. Golubkov, in: *Proceedings of XX International Congress on Glass*, Kyoto, Japan, September, 2004.
- [13] M. Hass, J.W. Davisson, H.B. Rosenstock, J. Babiskin, *Appl. Optics* 14 (5) (1975) 1128–1130.
- [14] L.B. Glebov, *Glass Sci. Technol.* 75 (C1) (2002) 73–90.
- [15] J. Lumeau, L. Glebova, L.B. Glebov, *Adv. Mater. Res.* 39–40 (2008) 395–398.
- [16] G.P. Souza, V.M. Fokin, E.D. Zanotto, J. Lumeau, L. Glebova, L.B. Glebov, *Micro and nanostructures in partially crystallized photo-thermo-refractive glass*, *Phys. Chem. Glasses: Eur. J. Glass Sci. Technol. B*, in press.
- [17] L. Glebova, J. Lumeau, M. Klimov, E.D. Zanotto, L.B. Glebov, *J. Non-Cryst. Solids* 354 (2008) 456–461.
- [18] S. Stević, R. Aleksić, N. Backovi, *J. Am. Ceram. Soc.* 70 (1101 C-264-C-265) (1987).
- [19] V. Mastelaro, E. Zanotto, *J. Non-Cryst. Solids* 194 (1996) 297–304.
- [20] J. Lumeau, A. Sinitskiy, L.N. Glebova, L.B. Glebov, E.D. Zanotto, *Method to assess the homogeneity of photosensitive glasses: application to photo-thermo-*

- refractive glass, *J. Non-Cryst. Solids*, in press, doi:10.1016/j.jnoncrysol.2009.05.054.
- [21] J.H. Simmons, K.S. Potter, *Optical Materials*, Academic Press, 2000. pp. 153–154.
- [22] J. Zwanziger, U. Werner-Zwanziger, E.D. Zanotto, E. Rotari, L.N. Glebova, L.B. Glebov, J.F. Schneider, *J. Appl. Phys.* 99 (2006) 083511.
- [23] F.C. Serbena, G.P. Souza, E.D. Zanotto, J. Lumeau, L. Glebova, L.B. Glebov, Paper Presented at ISNCS 2007 (Aracaju, Brazil), Paper P24, October 2007, to be submitted to the JNCS.
- [24] J. Selsing, *J. Am. Ceram. Soc.* 44 (1961) 419.
- [25] M.H. Sadd, *Elasticity: Theory, Applications, and Numerics*, Academic Press, 2005.